Available online at www.sciencedirect.com
SCIENCE DIRECT®
ELSEVIER
Physica E 34 (2006) 6–10
PHYSICA E
www.elsevier.com/locate/physe

Observations of nascent superfluidity in a bilayer two-dimensional electron system at $\nu_T = 1$

M. Kellogg[a], J.P. Eisenstein[a,*], L.N. Pfeiffer[b], K.W. West[b]

[a]*Condensed Matter Physics, California Institute of Technology, Pasadena, CA 91125, USA*
[b]*Bell Laboratories, Lucent Technologies, Murray Hill, NJ 07974, USA*

Available online 17 April 2006

Abstract

Single-layer longitudinal and Hall resistances have been measured in a bilayer two-dimensional electron system at $\nu_T = 1$ with equal but oppositely directed currents flowing in the two layers. At small effective layer separation and low temperature, the bilayer system enters an interlayer coherent state expected to exhibit superfluid properties. We detect this nascent superfluidity through the vanishing of both resistances as the temperature is reduced. This corresponds to the counterflow conductivity rising rapidly as the temperature falls, reaching $\sigma_{xx}^{CF} = 580(e^2/h)$ by $T = 35\,\text{mK}$. This supports the prediction that the ground state of this system is an excitonic superfluid.

PACS: 73.40.−c; 73.20.−r; 73.63.Hs

Keywords: Bilayer 2DES; Excitonic superfluidity; Quantum Hall effect

1. Introduction

A unique quantum state arises in double-layer two-dimensional electron systems (2DES) when the density n of electrons in each layer is equal to one-half of the degeneracy eB/h of the lowest spin-resolved Landau level *and* the layers are sufficiently close together so that interlayer Coulomb interactions are comparable to the intralayer interactions [1]. Under these conditions, in the low-temperature regime, the system achieves a lower total energy when electrons in one layer are configured opposite to the vacancies (holes) in the half-filled Landau level in the other layer. These electrons and holes bind together forming a system of interlayer excitons [2].

Unlike conventional excitons (conduction electrons bound to valence band holes), which are unstable against recombination into photons, the interlayer excitons in the present case consist of holes in one layer (a particle–hole transformation is performed on the half-filled Landau level) binding onto electrons in the half-filled Landau level in the other layer, and do not recombine. These stable excitons can theoretically condense into a BEC with well-understood properties [3–6], at least in the absence of disorder. Among the features anticipated is a superfluid mode manifesting as equal but oppositely directed dissipationless electrical currents flowing through the two layers—which can be thought of as arising from a superfluid flow of the interlayer excitons [2,7].

An alternate view of this state is one in which every electron exists in an identical superposition of the two layer states: $|\rightarrow\rangle = |\uparrow\rangle + e^{i\phi}|\downarrow\rangle$, with $|\uparrow\rangle$ denoting an electron located in the top layer, $|\downarrow\rangle$ an electron in the bottom layer, and ϕ a phase angle, arbitrary in the limit of zero interlayer tunneling. These superposition states are eigenvectors of pseudospin, lying in the xy-plane of pseudospin space. Since the pseudospins of all electrons are the same, the system is a ferromagnet, and may be viewed as a completely filled Landau level ($\nu_T = hn_T/eB = 1$ where n_T is the total density of the two layers combined) of pseudospin-aligned electrons [5,6]. As in an ordinary itinerant ferromagnet, the exchange energy is responsible

*Corresponding author.
E-mail address: jpe@caltech.edu (J.P. Eisenstein).

1386-9477/$ - see front matter
doi:10.1016/j.physe.2006.02.011

for enforcing this order. Spatial gradients in the phase ϕ represent pseudospin supercurrents or, equivalently, excitonic supercurrents.

This interlayer coherent state has been studied previously, exhibiting an integer quantized Hall effect (QHE) [8], an unusual textural phase transition [9], an extremely large peak in the interlayer tunneling conductance at zero interlayer bias [10], and precise quantization of the Hall component of Coulomb drag [11].

In the early QHE measurements [8,9], the longitudinal and Hall resistances were measured in the conventional way—the current was sent through the two layers going in the same direction. But if the currents were to be sent through the two layers going in opposite directions, a superflow of excitons should result (if the layers are close enough together) and be detectable as a vanishing of not only the longitudinal resistance, but also of the Hall resistance. In this paper we report on observations of this dramatic effect. Our results strongly support the existence of nearly dissipationless exciton transport at $\nu_T = 1$.

2. Experimental details

These experiments were conducted using a GaAs/AlGaAs heterostructure consisting of two GaAs wells 18 nm wide separated by a 10 nm wide $Al_{0.9}Ga_{0.1}As$ barrier. The as-grown electron density in each well is $5.4 \times 10^{10}\,\mathrm{cm}^{-2}$ with a low-temperature mobility of about $1 \times 10^6\,\mathrm{cm}^2/\mathrm{Vs}$. Using standard photolithographic techniques, we etched a $160\,\mu\mathrm{m} \times 320\,\mu\mathrm{m}$ mesa with seven arms extending out from it (see Fig. 1). Aluminum gates above and below the arms allow for in situ control over which layer each arm contacts [12]. Arms 1–4 make up the two Y-shaped projections at the opposite ends of the bar and are used for injecting current symmetrically into the layers; arms 5–7 are for probing the longitudinal and Hall voltages in the main mesa region. The longitudinal probes (5, 6) are spaced $160\,\mu\mathrm{m}$ apart, the width of the mesa, and so we are measuring along "one square". Large aluminum gates were also evaporated above and below the central mesa area allowing us to reduce the electron density in each well by as much as a factor of 2.5. The sample was thinned to $49\,\mu\mathrm{m}$ during processing. The tunneling resistance at resonance in zero magnetic field was measured to be $R_{\mathrm{tun}} \approx 100\,\mathrm{M}\Omega$.

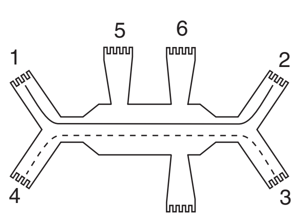

Fig. 1. A schematic illustration of the mesa region: arms 1–4 are for driving currents through the electron layers and arms 5–7 are for measuring the resulting voltages. For the counterflow configuration, a current is sent through the bottom layer by arms 1 and 2 (the solid line shows the route) and then an oppositely directed current goes through the top layer through arms 3 and 4 (the dashed line). Gate electrodes omitted for clarity.

A 2.3 Hz, 0.5 nA current is sent first through the bottom layer (via arms 1 and 2 shown in Fig. 1) and then redirected to go through the top layer (via arms 3 and 4) going either in the same direction (the parallel configuration) or in the opposite direction (the counterflow configuration). Because the interlayer coherent state exhibits enhanced tunneling [10], we measure the current before it enters the first layer and then after it has left the first layer but before entering the second layer—the difference between the two represents the loss due to the interlayer tunneling current. This loss is roughly 5 pA when the system is at $\nu_T = 1$, consistent with other measurements of the interlayer coherent tunneling in the sample. In the counterflow configuration, this will not affect the relative magnitudes of the currents in the layers, they will still carry equal but opposite currents despite the small tunneling leakage.

The voltages are measured in just one of the layers using arms (5, 6) and (6, 7). The longitudinal (Hall) voltage V_{xx} (V_{xy}) divided by the injected current, yields the longitudinal (Hall) resistance R_{xx} (R_{xy}). Superscripts $\|$ and CF indicate whether the current is in the parallel or counterflow configuration, respectively.

3. Data

Fig. 2 displays the primary result of this experiment. The main figure shows the Hall resistance at $n = 2.46 \times 10^{10}\,\mathrm{cm}^{-2}$ per layer and $T = 30\,\mathrm{mK}$ for both the parallel (dotted line) and counterflow (solid line) configurations. This density corresponds to $d/\ell = 1.55$ when calculated at $\nu_T = 1$, where $\ell = (\hbar/eB)^{1/2}$ is the magnetic length, and $d = 28\,\mathrm{nm}$ is the center-to-center spacing between the quantum wells. The ratio d/ℓ is the effective layer separation and

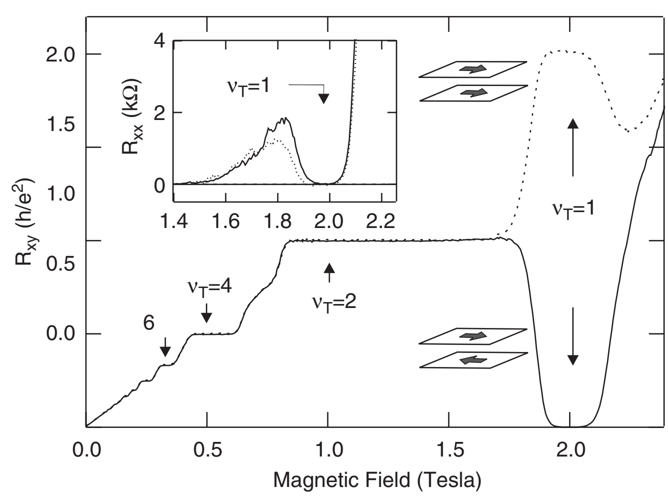

Fig. 2. Main figure shows the Hall resistance versus magnetic field in the parallel (dotted line) and counterflow (solid line) configuration for $n = 2.46 \times 10^{10}\,\mathrm{cm}^{-2}$ and $T = 30\,\mathrm{mK}$. The inset shows the longitudinal resistances. Voltages are measured in one layer only.

characterizes the relative importance of the inter- versus intra-layer Coulomb interactions.

Up to about $B = 1.8\,\mathrm{T}$ the layers behave independently and we see the usual quantum Hall effect in the single layer being measured, as though the second layer were not present. The direction of the current in the second layer is irrelevant and so $R^{\parallel}_{xy} = R^{\mathrm{CF}}_{xy}$. As the system enters the interlayer coherent state at $\nu_{\mathrm{T}} = 1$, at around $B = 2\,\mathrm{T}$, the direction of the current in the second layer splits the data: $R^{\parallel}_{xy}$ goes up to form a quantized plateau at $2h/e^2$ while R^{CF}_{xy} drops toward zero.

Notice that the plateau in the parallel configuration is at twice the expected value for filling factor one, this is because we define the resistance as the voltage divided by the current in a single layer, not the total current flowing through the bilayer.

The inset shows the longitudinal resistances $R^{\parallel}_{xx}$ and R^{CF}_{xx} under the same conditions, here just focusing on the region near $\nu_{\mathrm{T}} = 1$. Although not shown, the two are again identical at low fields. Contrary to the Hall resistance, they are also very similar in the interlayer coherent state. R^{CF}_{xx} (solid line) is a little larger than $R^{\parallel}_{xx}$ (dotted line) around $1.8\,\mathrm{T}$, which is where the sample is transitioning into the $\nu_{\mathrm{T}} = 1$ state. This is because of the strong interlayer Coulomb drag that occurs in the transition region [13]. When the sample is in the counterflow configuration, the two oppositely directed currents will exert a strong dragging force on one another that will increase R^{CF}_{xx} relative to $R^{\parallel}_{xx}$. Both $R^{\parallel}_{xx}$ and R^{CF}_{xx} go to zero at $\nu_{\mathrm{T}} = 1$, indicating that the $\nu_{\mathrm{T}} = 1$ state is dissipationless (in the zero temperature limit) in both the parallel and counterflow configurations.

Focusing on the resistances at precisely $\nu_{\mathrm{T}} = 1$, Fig. 3 shows the temperature dependence of the various quantities when the system is in the interlayer coherent state. Panel (a) shows $R^{\parallel}_{xx}$ (open circles) and $R^{\parallel}_{xy}$ (closed squares) for $d/\ell = 1.48$ for temperatures ranging from 35 to 400 mK. The Hall resistance never strays far from its quantized value $2h/e^2$, while the longitudinal resistance drops nearly three orders of magnitude, exhibiting straight line activated behavior $R^{\parallel}_{xx} = R_0 e^{-\Delta/2T}$ with energy gap $\Delta \approx 0.5\,\mathrm{K}$.

Panel (b) shows the same for the counterflow configuration, R^{CF}_{xx} (open circles) and R^{CF}_{xy} (closed squares). R^{CF}_{xx} is very similar to $R^{\parallel}_{xx}$, showing the same activated behavior with the same energy gap of $\Delta \approx 0.5\,\mathrm{K}$. But here R^{CF}_{xy} also drops precipitously as the temperature is lowered and at a very similar rate to the R_{xx} data.

More illuminating is the same data plotted as longitudinal conductivity $\sigma_{xx} = \rho_{xx}/(\rho^2_{xx} + \rho^2_{xy})$ shown in panel (c) [14]. Here the transport properties of the two different current configurations clearly and radically diverge as the temperature is lowered. The upward pointing triangles in the top half of panel (c) indicate the longitudinal conductivity in the counterflow configuration $\sigma^{\mathrm{CF}}_{xx}$; and the downward triangles in the bottom half represent $\sigma^{\parallel}_{xx}$. $\sigma^{\parallel}_{xx}$ goes to zero as the temperature goes to zero, again, in an activated fashion. This is precisely the behavior expected for the ordinary quantum Hall state. On the other hand, $\sigma^{\mathrm{CF}}_{xx}$ becomes dramatically larger as T is lowered. At 35 mK more than six orders of magnitude separate the conductivities of the two different current configurations. This behavior of $\sigma^{\mathrm{CF}}_{xx}$ is novel to 2DES systems. It suggests that there may be superfluid flow $\sigma^{\mathrm{CF}}_{xx} = \infty$ in the zero-temperature limit.

To investigate the dependence of the interlayer coherent state on the effective layer separation d/ℓ, we look at the evolution of R^{CF}_{xy} as d/ℓ is varied. In Fig. 4, R^{CF}_{xy} is measured at $T = 50\,\mathrm{mK}$ at differing values of d/ℓ and plotted versus the inverse of the total filling factor ν_{T}^{-1}. We vary d/ℓ at $\nu_{\mathrm{T}} = 1$ by symmetrically varying the layer density n. The topmost curve, with $d/\ell = 2.29$, shows the sample to be well out of the interlayer coherent state. The behavior seen is typical of the Hall resistance in a single layer 2DES. There is no distortion or feature at $\nu_{\mathrm{T}} = 1$,

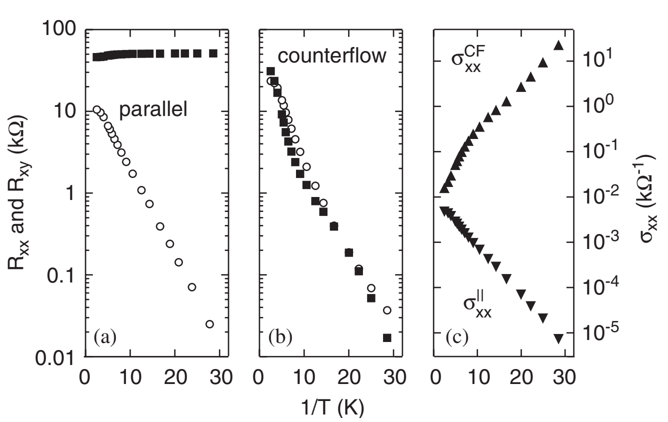

Fig. 3. Temperature dependence of the resistances (panels a and b) and conductivity (panel c) at $\nu_{\mathrm{T}} = 1$ for both parallel and counterflow configurations at $d/\ell = 1.48$. In (a) open circles represent $R^{\parallel}_{xx}$, closed squares $R^{\parallel}_{xy}$; in (b) open circles represent R^{CF}_{xx}, closed squares R^{CF}_{xy}. (c) shows the counterflow and parallel longitudinal conductivities, $\sigma^{\mathrm{CF}}_{xx}$ and $\sigma^{\parallel}_{xx}$, respectively.

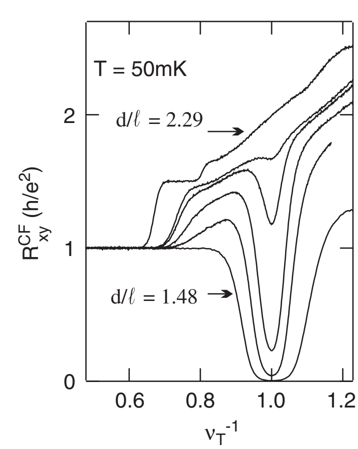

Fig. 4. Sample enters interlayer coherent state as evidenced by R^{CF}_{xy} dropping to zero as the effective layer separation d/ℓ is reduced. Figure shows R^{CF}_{xy} versus inverse filling factor ν_{T}^{-1} for $d/\ell = 2.29$, 1.75, 1.71, 1.66, 1.59, 1.48 all at $T = 50\,\mathrm{mK}$.

indicating a lack of correlation with the second layer. As d/ℓ is reduced, a dip begins to form at $\nu_T = 1$, becoming deeper and more fully developed as the layers are brought (effectively) closer together. By $d/\ell = 1.48$ there is a broad minimum that goes very near to zero indicating that the sample is now well within the interlayer coherent state. By interpolation, the minimum reaches half its uncorrelated value at $d/\ell = 1.70$, which may be thought of as the location of the phase boundary. This is consistent with observations of the phase boundary location as measured in prior Coulomb drag experiments [13].

4. Discussion

The view of this state as a BEC of interlayer excitons offers the most intuitive explanation of our observations, and so we focus on this interpretation. Our Hall resistance measurements at $\nu_T = 1$ in the counterflow configuration support the idea that the current is being carried not by isolated electrons in each layer, but by interlayer excitons. Because excitons are charge neutral, their motion will be unaffected by the magnetic field, and contrary to usual experience, the current flow will *not* be accompanied by a Hall voltage, as is dramatically displayed in Fig. 2. The superfluid nature of this exciton flow is indicated in the inset: the longitudinal resistance, and thus the dissipation, drops toward zero at $\nu_T = 1$. The bilayer system now resembles a superconductor: with vanishing longitudinal and Hall resistance, the conductivity goes toward infinity. In stark contrast is the parallel transport data in which the conductivity drops toward zero as the longitudinal resistivity does, as seen in the usual quantum Hall states.

However, as Fig. 3 shows, both the dissipation R_{xx}^{CF} and Hall resistivity R_{xy}^{CF} in the counterflow configuration remain finite at finite temperature. In the ideal case, both of these quantities should drop to zero (in linear response) for $T < T_{KT}$, where T_{KT} is the Kosterlitz–Thouless temperature [15,16]. Instead we find activated behavior.

In the ideal case, vortex-like charged excitations of the superfluid state, merons and anti-merons [5,6], exist only in bound pairs when $T < T_{KT}$, and both the longitudinal and Hall resistance should be identically zero (in linear response). Thus, one possible explanation for why we observe finite resistances could be that $T_{KT} < 30\,\mathrm{mK}$, and we have simply not gone below it. Ignoring disorder, this seems unlikely since many of the striking phenomena exhibited by the $\nu_T = 1$ state persist up to $\sim 300\,\mathrm{mK}$, a temperature quite consistent with estimates of T_{KT} [6]. In any case, it seems certain that disorder is very important in the regime of our experiments; the rapidly rising R_{xx} above $B \approx 2.05\,\mathrm{T}$ in Fig. 2 is one example of the strong evidence for this. Since merons and anti-meron vortices carry electrical charge, they couple strongly to disorder and might therefore exist individually even at very low temperatures [17]. If such individual vortices are weakly pinned, a finite population of them would exist at all temperatures and their motion could lead to thermally activated resistances in counterflow. Recent theoretical work has suggested that such a disordered system might exhibit glassy properties, with true superfluidity suppressed all the way to $T = 0$ [17–20]. This seems consistent with our observation that σ_{xx}^{CF} appears to rise without bound as $T \to 0$.

Being charge-neutral, excitons are not generally associated with an electrical conductivity, but rather with a diffusivity, D. In our case, a conductivity σ_{xx}^{CF} makes sense because we can apply, in effect, equal but opposite electric fields to the two layers and thus drive counterflowing electrical currents. The diffusivity D is defined via $j_x = D(\partial n/\partial x)$, where j_x is the number current density in the x-direction and n the exciton concentration. Setting $\partial n/\partial x = (\partial n/\partial \mu)(\partial \mu/\partial x)$, with μ the chemical potential, the diffusivity may be written in terms of the counterflow conductivity: $D = (\sigma_{xx}^{CF}/e^2)\partial\mu/\partial n$ where $\partial\mu/\partial n$ is the inverse of the density of states. If, for a rough estimate, we insert the density of states of the 2DES at zero magnetic field, we find $D \sim 5000\,\mathrm{cm}^2/\mathrm{s}$ at $T = 35\,\mathrm{mK}$ where, at $\nu_T = 1$, $\sigma_{xx}^{CF} \approx 580\,e^2/h$. This likely underestimates D since the 2DES is gapped at $\nu_T = 1$ and its density of states may be very small. In any case, this value for D, while clearly uncertain, far exceeds those recently reported for optically generated exciton gases at temperatures of a few Kelvin [21].

5. Conclusion

We have observed vanishing Hall and longitudinal resistances in the counterflow current configuration of a bilayer two-dimensional electron system at $\nu_T = 1$. The conductivity in the counterflow channel increases dramatically as the temperature is reduced, measuring $\sigma_{xx}^{CF} \approx 580\,e^2/h$) at $T = 35\,\mathrm{mK}$. Both R_{xx}^{CF} and $R_{xx}^{\parallel}$ show activated behavior with energy gap $\Delta \approx 0.5\,\mathrm{K}$. The origin of this energy gap is not well understood and warrants further investigation, however, it is not inconsistent with a description of the ground state of the system as a disordered Bose–Einstein condensate of excitons.

Acknowledgments

We thank Allan MacDonald for helpful discussions. This work was supported by the NSF under Grant no. DMR-0242946 and the DOE under Grant no. DE-FG03-99ER45766.

References

[1] Throughout this paper we discuss only the case of balanced bilayer systems, i.e. those with equal densities in the two layers. For the unbalanced case see, for example, I.B. Spielman, M. Kellogg, J.P. Eisenstein, L.N. Pfeiffer, K.W. West, Phys. Rev. B 70 (2004) 081303.
[2] A.H. MacDonald, Physica B 298 (2001) 129.
[3] X.G. Wen, A. Zee, Phys. Rev. Lett. 69 (1992) 1811.
[4] Z.F. Ezawa, A. Iwazaki, Phys. Rev. B 47 (1993) 7295.

[5] K. Yang, et al., Phys. Rev. Lett. 72 (1994) 732.
[6] K. Moon, et al., Phys. Rev. B 51 (1995) 5138.
[7] A.H. MacDonald, E.H. Rezayi, Phys. Rev. B 42 (1990) 3224.
[8] J.P. Eisenstein, G.S. Boebinger, L.N. Pfeiffer, K.W. West, S. He, Phys. Rev. Lett. 68 (1992) 1383.
[9] S.Q. Murphy, J.P. Eisenstein, G.S. Boebinger, L.N. Pfeiffer, K.W. West, Phys. Rev. Lett. 72 (1994) 728.
[10] I.B. Spielman, J.P. Eisenstein, L.N. Pfeiffer, K.W. West, Phys. Rev. Lett. 84 (2000) 5808;
I.B. Spielman, J.P. Eisenstein, L.N. Pfeiffer, K.W. West, Phys. Rev. Lett. 87 (2001) 036803.
[11] M. Kellogg, I.B. Spielman, J.P. Eisenstein, L.N. Pfeiffer, K.W. West, Phys. Rev. Lett. 88 (2002) 126804.
[12] J.P. Eisenstein, L.N. Pfeiffer, K.W. West, Appl. Phys. Lett. 57 (1990) 2324.
[13] M. Kellogg, J.P. Eisenstein, L.N. Pfeiffer, K.W. West, Phys. Rev. Lett. 90 (2003) 246801.
[14] We take $\rho = R$ as the longitudinal voltage probes are spaced one square apart.
[15] J.M. Kosterlitz, D.J. Thouless, J. Phys. C 6 (1973) 1181.
[16] See the chapter by S.M. Girvin, A.H. MacDonald, in: S. Das Sarma, A. Pinczuk (Eds.), Perspectives in Quantum Hall Effects, Wiley, New York, 1997.
[17] H.A. Fertig, J.P. Straley, Phys. Rev. Lett. 91 (2003) 046806.
[18] D.N. Sheng, L. Balents, Z. Wang, Phys. Rev. Lett. 91 (2003) 116802.
[19] Z. Wang, Phys. Rev. Lett. 94 (2005) 176804.
[20] A. Stern, S. Das Sarma, M.P.A. Fisher, S.M. Girven, Phys. Rev. Lett. 84 (2000) 139.
[21] Z. Voros, R. Balili, D. Snoke, L.N. Pfeiffer, K.W. West, cond-mat/0504151.